JOURNAL OF MATERIALS SCIENCE **34** (1999) 811–820

A study of high-temperature precipitation in Al–Mg–Si alloys with an excess of silicon

D. G. ESKIN*, V. MASSARDIER, P. MERLE
G.E.M.P.P.M., Institut National des Sciences Appliquées de Lyon, 20 av. Albert Einstein, Bât. 502, 69621 Villeurbanne, France
E-mail: eskin@ultra.imet.ac.ru

The high-temperature decomposition phenomena were examined for two Al–Mg–Si alloys with an excess of silicon. The kinetics of precipitation were studied by transmission electron microscopy and by measurement of the thermoelectric power in the temperature range from 300 to 525 °C. It was shown that decomposition occurs either at 300–400 °C by the precipitation of intermediate β' phase (different structures are possible depending on the alloy), which is then gradually replaced by the equilibrium β phase or, between 400 and 500 °C, by direct precipitation of the β phase from the supersaturated solid solution. The precipitation of silicon was also observed. At 300–350 °C, a near equilibrium in composition solid solution can coexist with Mg_2Si phases out of equilibrium. Structures of intermediate phases and their orientation relationships with the matrix are given. The diagram of isothermal precipitation is constructed as an S-curve.

1. Introduction

Al–Mg–Si alloys represent a large group of light materials that are most commonly used for extrusion. These alloys are usually subjected to artificial aging to obtain increased strength. The properties of these alloys are highly dependent on the distribution of the alloying elements, Mg and Si, in the matrix and in precipitates. The nature of precipitation hardening in these alloys is well established [1].

For the alloys without an excess of silicon, the decomposition of the solid solution obtained after quenching from the solutionizing temperature is generally believed to be as follows: supersaturated solid solution $\Rightarrow$ vacancy-rich zones $\Rightarrow$ β'' coherent precipitates $\Rightarrow$ β' semi-coherent precipitates $\Rightarrow$ β (Mg_2Si) incoherent precipitates.

The structure of the coherent β'' phase is monoclinic, although there is some discussion about the lattice parameters. However, the structure of the β' phase has not been well established. Jacobs [2] reported that the β' phase had a hexagonal structure with $a = 0.705$ nm and $c = 0.405$ nm and appeared as rod-shaped precipitates. He also suggested that, upon growth, these rods lost coherency along their length and acquired the hexagonal lattice cell with $a = 0.705$ nm and $c = 1.215$ nm. On further annealing, the β' phase transformed to the equilibrium Mg_2Si cubic phase ($a = 0.639$ nm). However, recent high-resolution electron microscopy studies showed the existence of several types of β' precipitates, which are listed in Table I.

The main problem is that observations were made using different alloys and particular annealing modes, without any attempt to follow the kinetics and explain why the Mg_2Si phase acquires different structures and how one structure may transform into another. Recently, the attention of scientists has been attracted to the problem of high-temperature precipitation in Al–Mg–Si alloys. This demand has arisen from the industrial need to optimize the structure of ingot before extrusion. Therefore, it is necessary to know how the structure changes upon cooling and high-temperature anneals. There are few publications dealing with this problem.

A thorough analysis of precipitation reactions in an Al–1 wt % Mg_2Si alloy was done by Westengen and Ryum [7]. They examined by TEM samples cooled at different rates, quenched, and annealed or directly annealed at temperatures up to 450 °C. After direct annealing at 450 °C, only the equilibrium β particles were observed, these being of a plate shape and collected in strips along the rolling direction. This observation was explained by impurities (Fe, Mn-based particles) acting as nucleation sites for β plates. At 350 °C, precipitation starts from the formation of rod-like particles of the semi-coherent β' phase, and then the equilibrium Mg_2Si particles (plates and cubes) are formed with the orientation relationship $(001)_\beta \| (001)_m$; $\langle 100 \rangle_\beta \| \langle 100 \rangle_m$. These authors have found that the semi-coherent phase is that reported by Jacobs [2]. At 350 °C, which is below the solvus of the β' phase, the semi-coherent phase

*Occupied a post-doctoral position at INSA de Lyon. Originally from Baikov Institute of Metallurgy, 49 Leninskii prosp., 117334 Moscow, Russia.

TABLE I Crystal structures of the β' phase

Lattice parameters, nm					Composition of an alloy, wt %			
a	*b*	*c*	Crystal structure	Mg:Si atomic ratio in precipitates	Mg	Si	Annealing temperature, °C	Refs.
0.705		0.405	Hexagonal	0.44	0.76	0.44	250 (10 min)[a]	[2, 3]
0.405		0.67	Hexagonal (A)	0.28	0.635	0.765	250 (3.3 h)	[4]
0.407		0.405	Hexagonal	1.68	0.635	0.365	250 (33 h)	[5]
0.684	0.793	0.405	Orthorhombic (B)	0.4	0.635	0.765	250 (3.3 h)	[4, 6]
1.04		0.405	Hexagonal (C)	0.83	0.635	0.765	250 (33 h)	[4]
0.672	0.787	0.405	Orthorhombic	1.21	0.64	0.81	250 (1 h)	[6]

[a]Samples were previously aged at room temperature for 1 week.

is formed on dislocations and after long annealing, β' goes into solution, whereas β plates start to grow. Note that the density of β particles, after the dissolution of β' has been completed, is nearly the same as after direct annealing at 450 °C. This has been interpreted as evidence of independent β precipitation. A similar pattern has been observed when annealing at 250 °C is performed, although the dissolution of β' and the formation of β are now very slow processes [7].

Lastly, in Al–Mg–Si alloys with an excess of Si, it is important to take into account the precipitation of silicon and the change in the Mg:Si ratio during the precipitation kinetics. Maruyama *et al.* [8] studied the effect of silicon addition on the composition and structure of fine precipitates in two alloys, namely, Al–0.63% Mg–0.35% Si (stoichiometry) and Al–0.64% Mg–0.81% Si (excess of silicon). The alloys were solution treated at 550 °C for 30 min and then annealed at 250 °C (1 h) and 350 °C (2 h). After annealing at 250 °C, both alloys contained two types of the β' phase (hexagonal, $a = 0.407$ nm and $c = 0.405$ nm [5], and orthorhombic [6]). Annealing at 350 °C produced the equilibrium β phase and silicon. Using a field emission TEM with an energy dispersive X-ray spectroscope, Maruyama *et al.* determined the composition of the precipitates. The Mg:Si atomic ratio of the β' and β phases was found to be 1.75 and 2.10 in the stoichiometric alloy and 1.21 and 2.13 in the alloys with excess silicon. It should be noted that different Mg:Si atomic ratios of the β' phase composition in both alloys did not affect the crystal structure of the precipitates, which was found to be the same. Moreover, it was observed that in the same alloy, the composition of the two types of β' precipitates having different structures is similar. It should be noted that the coexistence of intermediate phases with different structures may reflect the stage of transformation from one phase to another. However, this kinetic problem is still unclear. From this work [8], we can conclude that in the presence of excess silicon in the alloy, the intermediate precipitates are enriched in this element and release it when their structure develops towards the equilibrium phase.

In this context, the aim of the present study is to trace the evolution of structure and phase composition of Al–Mg–Si alloys with an excess of silicon, as these alloys are known to provide the highest hardening effect upon aging [1].

2. Experimental procedures

2.1. Materials and thermal treatments

Two Al–Mg–Si alloys (alloy *1* representing a 6351 commercial alloy and a ternary alloy *2*) with different concentrations of Mg and Si supplied by Péchiney-Voreppe were examined. The second alloy was used as a reference, and its behavior was examined at only two temperatures, 350 and 450 °C. The compositions of the alloys are given in Table II. Specimens were cut from rolled sheets 1 mm thick.

Both alloys were solution treated at 550 °C for 1 h in a salt bath. Isothermal anneals were performed in salt baths in the temperature range of 300 to 525 °C, with direct quenching to the temperature of the annealing.

To prevent the loss of Mg during high-temperature anneals at over 400 °C, the specimens were put inside open-top quartz ampules and, after annealing, the surface layer, depleted of Mg, was removed from both sides by grinding. We also verified the change of the bulk composition of alloys annealed at 550 °C (1 h), 300 °C (173 h), and 400 °C (600 h). A slight decrease in the bulk content of Mg was only observed after 600 h at 400 °C.

2.2. Experimental techniques

To study the kinetics of precipitation during annealing in the temperature range from 300 to 525 °C, transmission electron microscopy with selected-area diffraction (TEM) and thermoelectric power (TEP) measurements was used.

The principle of TEP method is to measure the low voltage (ΔV) arising from the Seebeck effect between two junctions of the sample with aluminium blocks. The temperatures of these junctions are T and T + ΔT, respectively. This technique has been described in a previous paper [9] and gives the relative TEP of the alloy with respect to aluminium (ΔS). This relative TEP is given by the ratio $\Delta S = \Delta V/\Delta T$. The experimental plots present the variation in TEP, namely $\Delta(\Delta S) = \Delta S_t - \Delta S_0$, where ΔS_0 is the TEP of the initial state and ΔS_t is the current value of TEP.

TABLE II Compositions of examined alloys

Alloy	Si, wt %	Mg, wt %	Fe, wt %	Mg_2Si, wt %	Excess of Si, wt %
1	0.89	0.68	0.18	1.07	0.50
2	0.9	0.9	—	1.42	0.38

TEP is sensitive to the variation in the composition of the solid solution. For example, at room temperature, the presence of Mg in the solid solution greatly increases the TEP ($\Delta S = 2.4\,\mu$V/K wt %), Si has a slight negative effect ($\Delta S = -0.74\,\mu$V/K wt %), and Fe strongly decreases the TEP ($\Delta S = -8\,\mu$V/K wt %) [9]. In addition, the formation of coherent and semi-coherent precipitates with asymetrical shapes (needles and rods of the β'' and β' phases in Al–Mg–Si alloys) produces an additional TEP decrease [10]. In contrast, the formation of incoherent equilibrium phases (assuming that the volume fraction of these phases is less than 10%, which is typical of the precipitation from the supersaturated solid solution) has no additional effect on the magnitude of TEP.

Therefore, as has been well established for the preciptation kinetics in Al–Mg–Si alloys, the precipitation of the semi-coherent β' phase results in a TEP decrease. When growth and coherency loss of β' particles occurs, the TEP increases and finally stabilizes with the formation of the equilibrium β phase.

It was discovered that the technique of annealing can affect the TEP variations. The usually adopted technique is to accumulate the annealing time with intermediate quenching in water and subsequent TEP measurement (interrupted annealing). However, starting from particular annealing times at high temperatures (above 400 °C), the TEP magnitude is different for interrupted and continuous anneals. To avoid this artifact, each point for isothermal kinetics at high temperatures was obtained individually rather than by accumulating the time of annealing.

The identification of phases formed during the anneals was carried out by analysing the selected-area electron diffraction patterns (SAEDP). TEM observations were performed with a JEOL-200CX electron microscope at an operating voltage of 200 kV.

Thin foils were prepared in a Tenupol-3 setup using a 70% CHO_4 and 30% HNO_3 electrolyte cooled below −20 °C. The operating voltage was 10–20 V with a current density of 200 mA.

When calculating EDP, all available data on the structure of β' and β phases was used. Note, however, that sometimes diffraction patterns, which could hardly be interpreted in terms of reported structures were obtained. As there are no kinetic studies of high-temperature precipitation, it is quite possible that some intermediate structures are still unknown.

3. Results

3.1. Identification of phase composition by transmission electron microscopy

Using known data [7, 8, 10, 11], we can expect that the decomposition of the supersaturated solid solution may start with the precipitation of an intermediate β' phase at temperatures below 400 °C. The decomposition at higher temperatures should start from direct precipitation of the equilibrium β phase.

To clarify the precipitation kinetics at 300 and 350 °C, we examined, by TEM, the evolution of phase composition during the annealing of alloy *1* at 300 °C (4 min, 2 h, 7.5 h, 87 h, and 173 h) and alloy *2* at 350 °C (15 min, 1 h, 3 h, 7 h, and 29 h). These times of annealing were selected using characteristic points deduced from the TEP curves (see section 3.2).

The summary of observed phase composition is given in Table III. The orientation relationships found in this study are illustrated in Fig. 1.

When designating an intermediate phase, we used indices suggested by Matsuda *et al.* [4]. The indices C and A for the metastable phase reflect the different structure of this phase. The C-type is the hexagonal phase with lattice parameters $a = 1.04$ nm and $c = 0.405$ nm, and the A-type is also hexagonal but with lattice parameters $a = 0.405$ nm and $c = 0.67$ nm. As the structure of the metastable phase gradually changes during annealing, the identification can be performed only with some ambiguity. For example, SAEDPs of alloy *1* annealed for 4 min show streaks and blurred reflections produced from fine needle or thin rod-shaped precipitates, Fig. 1a. We attributed these reflections to a semi-coherent phase with parameters close to that of β'_C, as the precipitation of a coherent phase is not expected at such a high temperature.

In alloy *1*, the precipitation at 300 °C starts with the formation of very fine elongated β' particles of the C-type (annealing for 4 min, Fig. 2a), which then (annealing for 2 h, Fig. 2b) continue to grow. After 7.5 h of annealing, large rather incoherent precipitates of the β' particles (Fig. 2c) and the precipitation of silicon in a form of either faceted particles (Fig. 3d) or uneven-shaped plates were observed. Because of the size of the Si particles obtained after this treatment, it is clear that the precipitation of silicon starts much earlier, indeed from the very beginning of annealing. However, the precipitation density of Si particles is low, and they can hardly be noticed against the background of numerous

TABLE III Phase composition of the alloys *1* and *2* upon annealing at 300 °C and 350 °C, respectively

Time	Alloy *1*	Time	Alloy *2*
4 min	β'_C $(001)_{Al} \parallel (001)_p$; $\langle 100\rangle_{Al} \parallel \langle 1\bar{2}0\rangle_p$ or $\langle 100\rangle_{Al} \parallel \langle 3\bar{1}0\rangle_p$	15 min	β'_A $\langle \bar{2}21\rangle_{\beta'} \parallel \langle 100\rangle_{Al}$; $(\bar{1}\bar{1}0)_{\beta'} \parallel (001)_{Al}$ $\langle 200\rangle_{\beta'} \parallel \langle 100\rangle_{Al}$; $(011)_{\beta'}$ 4–5° $(010)_{Al}$
2 h	β'_C $(001)_{Al} \parallel (001)_p$; $\langle 100\rangle_{Al} \parallel \langle 1\bar{2}0\rangle_p$ or $\langle 100\rangle_{Al} \parallel \langle 3\bar{1}0\rangle_p$	1 h	β'_A
7.5 h	β'_C $(001)_{Al} \parallel (001)_p$; $\langle 100\rangle_{Al} \parallel \langle 1\bar{2}0\rangle_p$ Si, β'_B	3 h	β'_A, Si
87 h	β, Si	7 h	β, β'_A, Si
173 h	β, Si	29 h	β, Si, β'_A

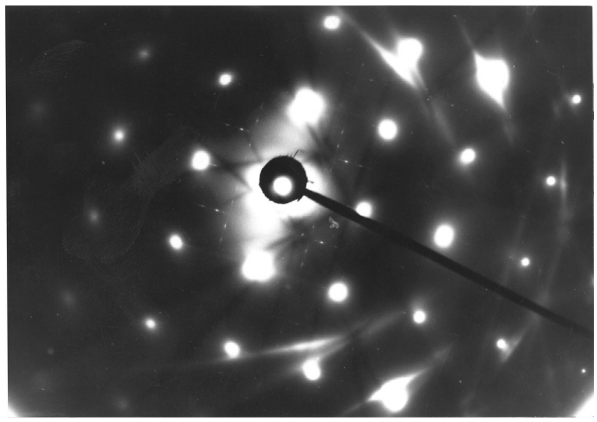

(a)

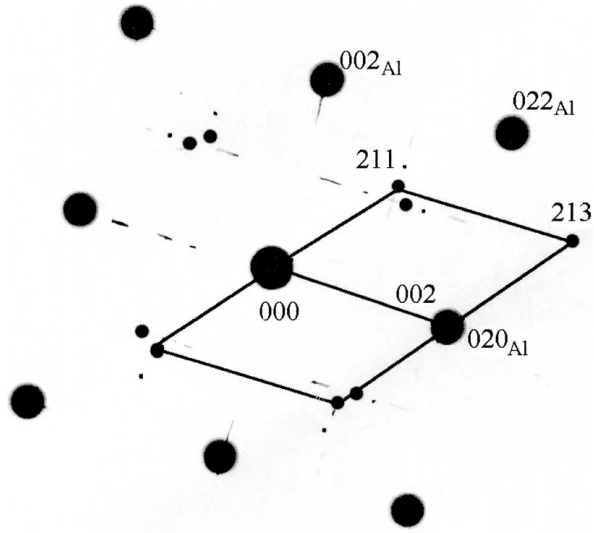

(b)

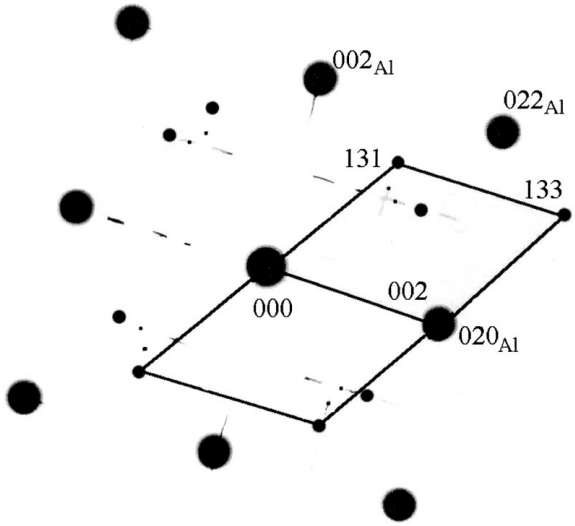

(c)

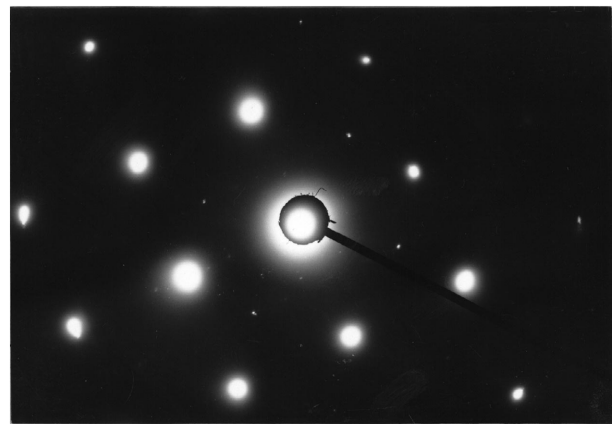

(d)

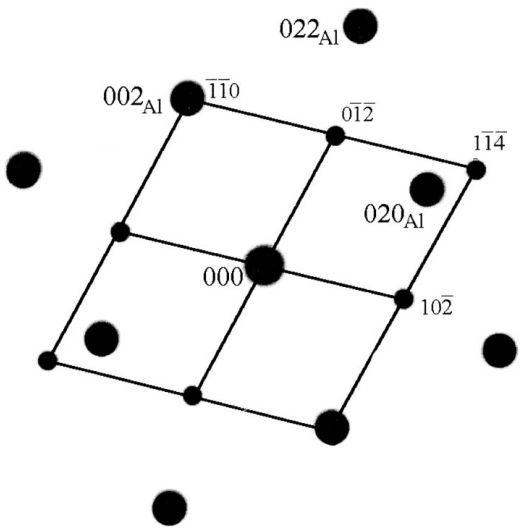

(e)

(f)

Figure 1 Electron diffraction patterns from β' particles and indiced schemes: *a*, *b*, alloy *1* (300 °C, 2 h) $\langle 1\,\bar{2}0\rangle_{\beta'} \parallel \langle 100\rangle_{Al}$; $(001)_{\beta'} \parallel (001)_{Al}$, *c*, alloy *1* (300 °C, 2 h) $\langle 3\,\bar{1}0\rangle_{\beta'} \parallel \langle \bar{1}00\rangle_{Al}$; $(001)_{\beta'} \parallel (001)_{Al}$ (β' phase of the C-type), *d*, *e*, alloy *2* (350 °C, 15 min) $\langle 2\,\bar{2}1\rangle_{\beta'} \parallel \langle 100\rangle_{Al}$; $(\bar{1}\,10)_{\beta'} \parallel (001)_{Al}$; *f*, *g*, alloy *2* (350 °C, 15 min) $\langle \bar{2}00\rangle_{\beta'} \parallel \langle 100\rangle_{Al}$; $(011)_{\beta'}$ 4–5 ° $(010)_{Al}$ (β' phase of the A-type) (*continued*).

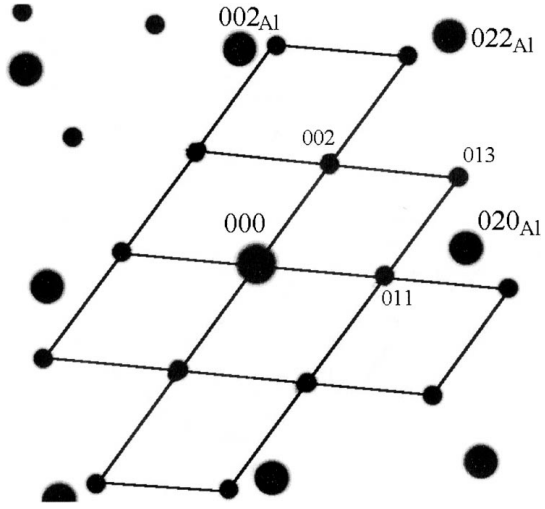

(g)

Figure 1 (*continued.*)

β' particles. Only after all particles completed their growth, could diffraction patterns from separate silicon precipitates be obtained.

The structure of alloy *1* dramatically changes after annealing for 87 h, as shown in Fig. 2e and f. One can observe fine cubic and plate-like precipitates that, judging by electron diffraction patterns, can be unambiguously attributed to the equilibrium β phase. Also seen here are the precipitates of Si and some coarser plate and rod-shaped precipitates, which were not interpreted. On further annealing, a coarsening of the structure with the same phase composition is obtained.

In the case of alloy *2* (Fig. 3, Table III), the decomposition of the supersaturated solid solution at 350 °C starts with the precipitation of the β' phase of the A-type (15 min and 1 h) in a form of rods, Figs 3a and 3b. Two orientation relationships mentioned in Table III were observed at early stages of decomposition. The indiced representations of relevant electron diffraction patterns are given in Fig. 1d to g. Silicon particles were revealed after annealing for 3 h as shown in Fig. 3c. The equilibrium β phase was observed after 7 h of annealing (Figs 3d and e) alongside coarse plate-like β' precipitates and Si particles. On further annealing, we observed precipitation of the β phase on fragmented coarse rods of β' phase (Fig. 3f) and tight connection between Si and β' precipitates when we obtained diffraction patterns of different phases from one agglomerate.

Therefore, in conclusion, although the structure of the intermediate phase may be different, the evolution of the microstructure at considerably high temperatures has some common features in both alloys. The decomposition starts with the precipitation of rod-shaped particles of the β' phase; these particles grow; after several hours of annealing, large particles of silicon are clearly seen; and on further annealing, the structure with compact particles of the equilibrium β phase is observed (although coarse particles with structures, close to those of β'-type phases can also be observed). It is noteworthy that particles of an intermediate phase, which are still called β', seem to lose the coherence bond with the matrix quite rapidly. According to TEM images, it happens after 3 h at 300 °C and 1 h at 350 °C.

3.2. Experimental results on the kinetics of precipitation

Now, knowing the phase composition of precipitates in our alloys, examination of decomposition kinetics in the entire temperature range, from 300 to 525 °C can proceed. These kinetic studies were performed by measuring the variation of thermoelectric power. The results are given in Fig. 4.

One can easily see that nothing happens at 525 °C; the TEP remains virtually unchanged. However, starting from 500 °C and below, considerable TEP variations, which are different at various temperature ranges, are observed. From 400 to 500 °C, the TEP decreases and, finally, equalizes. Such behavior is typical of the precipitation of only one phase, the formation of which depletes the solid solution of magnesium and thus decreases TEP. Taking into account reference data [7, 8], it is suggested that in this temperature range, this is the equilibrium β phase.

It should be noted that at 400 °C, there is a very rapid initial TEP decrease, which can reflect the precipitation of a metastable β' phase (with a negative "intrinsic" effect) even at this temperature.

In the temperature range from 300 to 350 °C, the TEP evolution shows a rapid decrease, which is much more pronounced than at 400 °C, then a TEP increase, and a sort of "maximum," after which the curve slightly decreases and becomes stable.

At all annealing temperatures, the TEP curve finally stabilizes, which can be attributed to the end of precipitation and to the achievement of the equilibrium or nearly equilibrium solid solution concentration. Obviously, the time required for this stabilization increases when the temperature decreases and is approximately equal to 10^4, 2×10^3, 9×10^2, 2×10^2, 8×10^1 and 2×10^1 min at 300, 350, 400, 450, 475, and 500 °C, respectively.

4. Discussion

4.1. Interpretation of the TEP results

Taking into account reference data [10, 11], possible TEP variations in Al–Mg–Si alloys can be suggested, as demonstrated in Fig. 5. The curve reflecting the direct precipitation of the equilibrium phase from the solid solution, without the formation of intermediate phases is not placed here. This curve is a classic example with a TEP decrease followed by a stabilization (like TEP curves at 450 and 475 °C in Fig. 4). In Fig. 5, curve *1* reflects only solid-solution effects due to the precipitation of intermediate Mg_2Si-based phases with an increase of the Mg:Si ratio. Upon precipitation of the Mg- and Si-containing phase from the supersaturated solid solution, the latter becomes gradually depleted of these elements, approaching the equilibrium composition at a given annealing temperature. As the effect of magnesium on TEP is much higher than that of silicon, we observe a gradual TEP decrease. Curve *2* shows the case observed by Dafir [10] and Seyed *et al.* [11], when the precipitation of a semi-coherent β' phase was accompanied by a much more pronounced TEP decrease than if it was due only to the variation of the composition of the solid

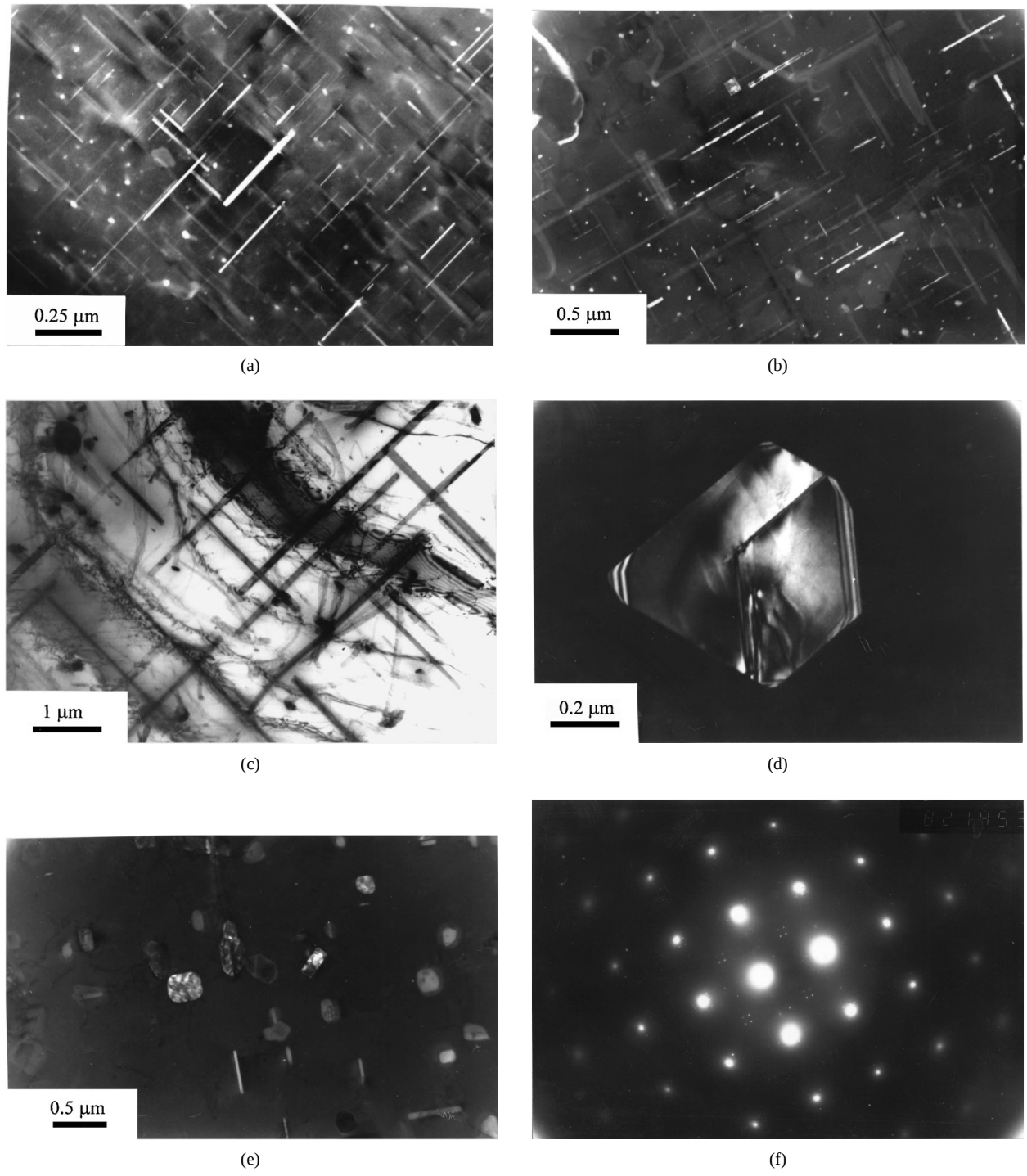

Figure 2 TEM images of the alloy *1* annealed at 300 °C for 4 min (a), 2 h (b), 7.5 h (c, d) and 87 h (e, f): *a*, *b*, β' particles (dark field); *c*, β' particles; *d*, Si (dark field); *e*, β particles (dark field); *f*, corresponding SAEDP $(001)^*_{Al}$ and $(100)^*_{\beta}$.

solution. This additional decrease results from the negative "intrinsic" effect of β' precipitates and, though well experimentally established and confirmed, has not been completely explained. Curve *2* shows also the transformation of the semi-coherent phase to the equilibrium one. During this transformation, the TEP increases and finally equalizes (compare with the curve for alloy *1* at 400 °C in Fig. 4). Lastly, curve *3* corresponds to our experimental curves, which exhibit a maximum before the final stabilization. After the initial sharp TEP decrease due to the negative intrinsic effect of the β' precipitates, the TEP increase can be attributed to the fact that as β' precipitates grow, they reach a critical size after which their intrinsic effect vanishes as a result of a gradual loss of coherency along their length. Then, the curve passes a maximum, which reflects the presence in the structure of an intermediate phase with nearly incoherent interfaces but nonequilibrium composition, or the beginning of the formation of the equilibrium phase. Finally, the curve equalizes, which testifies that the structure comprises a nearly equilibrium solid solution and incoherent phases with the stoichiometric Mg_2Si composition.

These speculations show that the interpretation of TEP curves requires the knowledge of phase composition obtained by direct measurements. At the same time,

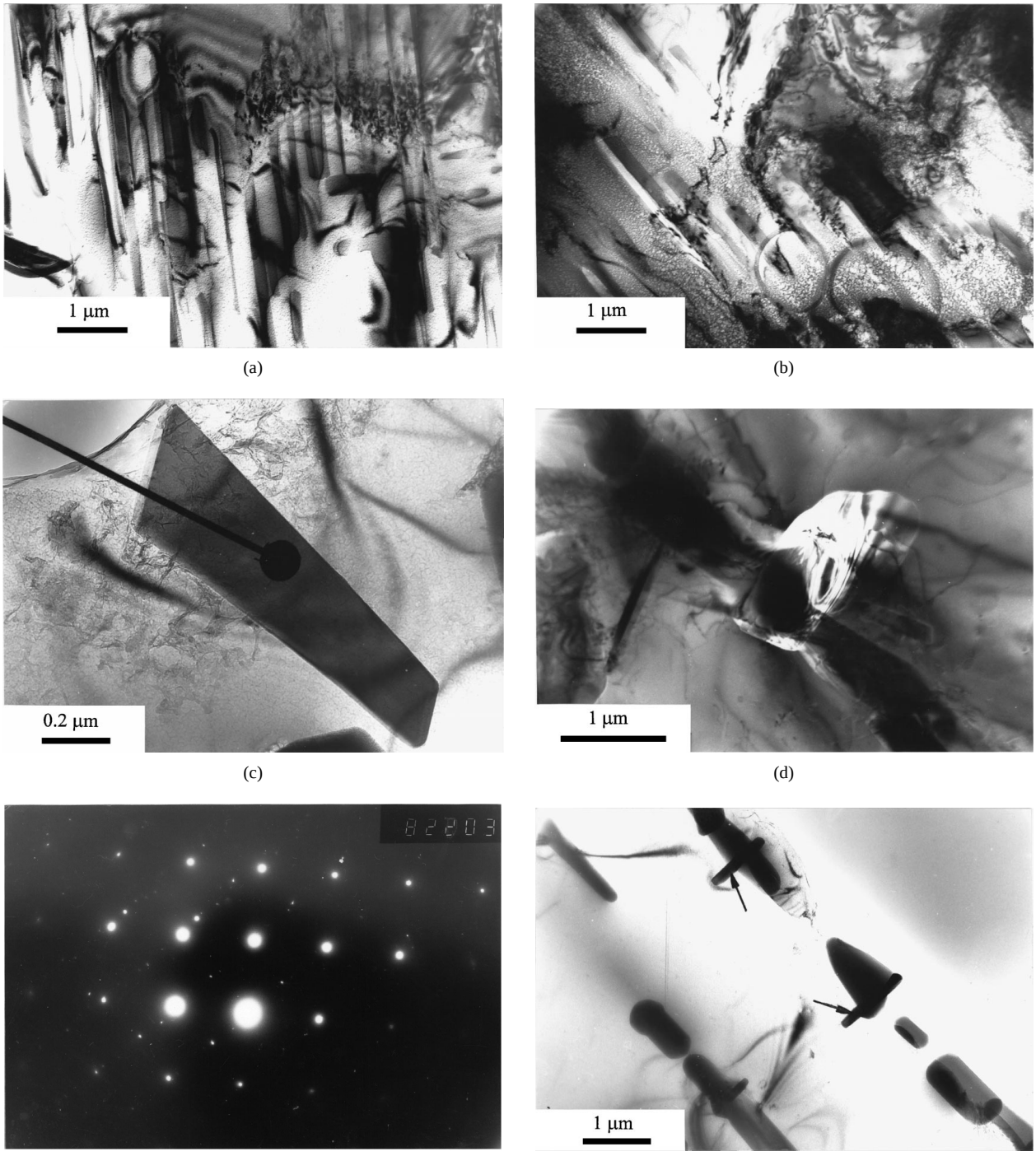

Figure 3 TEM images of alloy *2* annealed at 350 °C for 15 min (a), 1 h (b), 3 h (c), 7 h (d, e) and 29 h (f): *a*, *b*, β' particles; *c*, Si particle; *d*, β particle (dark field); *e*, corresponding SAEDP $(100)^{*}_{\beta}$ and $(001)^{*}_{Al}$; *f*, precipitation of the β phase on fragmented β' rods (pointed by arrows).

the TEP technique can be very sensitive to the solid-state transformations and can be successfully used for kinetics studies.

4.2. Correlation of TEP and TEM results

To explain the TEP variations at 300 °C (alloy *1*), the following model of precipitation is suggested, assuming some known facts: (1) the metastable β' phase gradually changes its structure and composition being initially enriched in silicon [8] and (2) the transition between the metastable phase and the equilibrium phase may occur by independent processes (dissolution of β' and precipitation of β) [7].

The precipitation of the metastable β' phase (the C-type) and Si starts very rapidly at 300 °C (decrease in TEP) (Figs 2a and 4). This β' phase changes during growth (Fig. 2c), and gradually dissolves (increase in TEP). A certain amount of silicon is simultaneously released from this phase and precipitates, forming additional Si particles (Fig. 2d). This release of silicon upon increasing Mg:Si ratio in intermediate Mg_2Si-based phases can also contribute to the increasing slope of the "maximum." Then the precipitation of the equilibrium β phase (Fig. 2e, and f) begins, decreasing and finally stabilizing the TEP (Fig. 4).

We can suggest that in the case of alloy *2* the maximum observed on the TEP curve at 350 °C matches

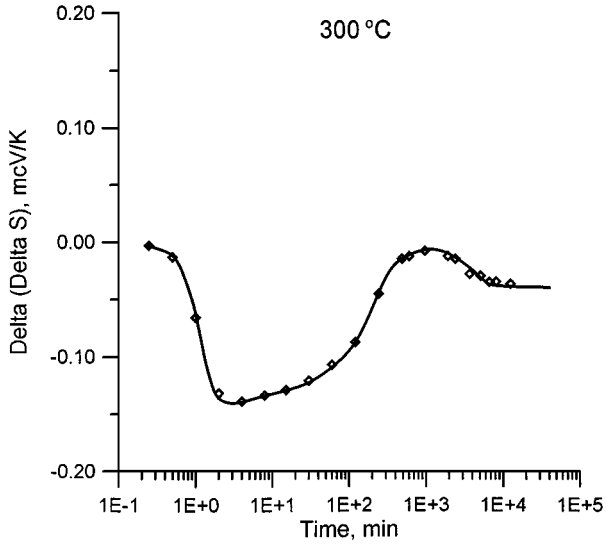

(a)

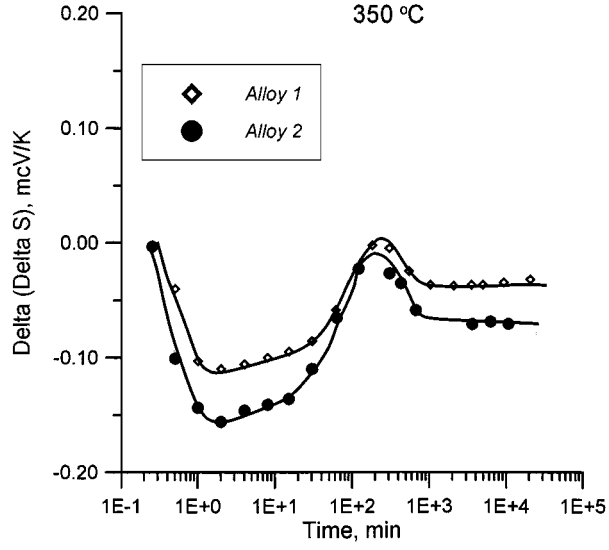

(b)

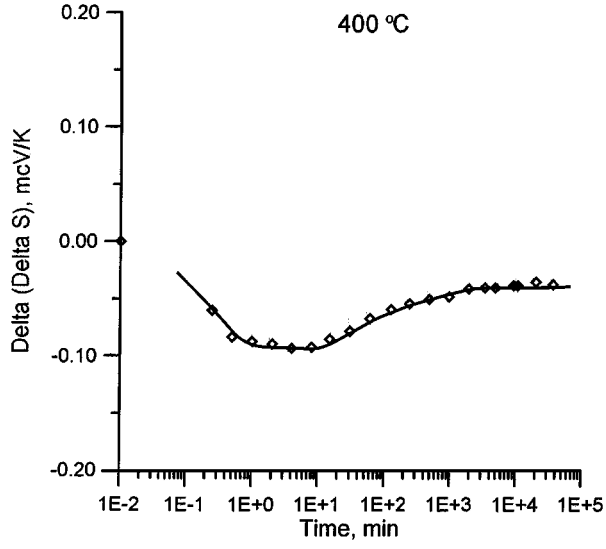

(c)

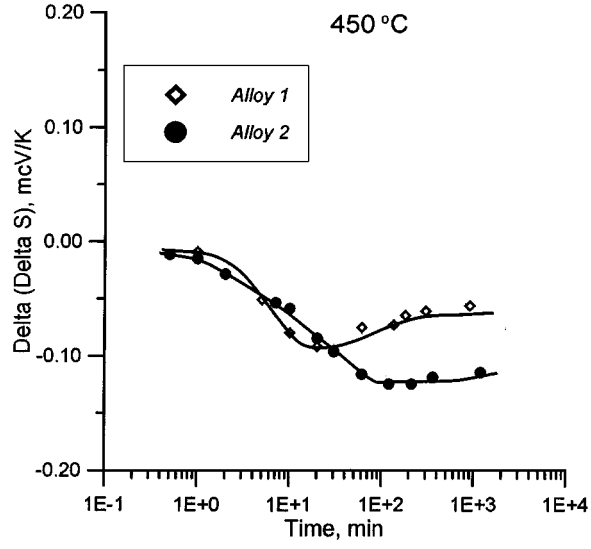

(d)

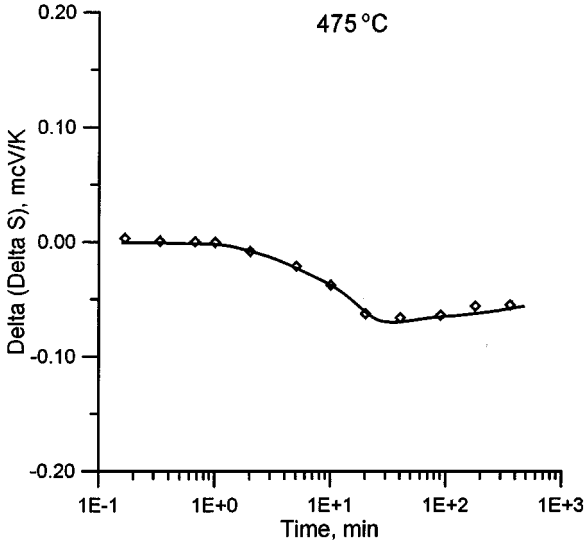

(e)

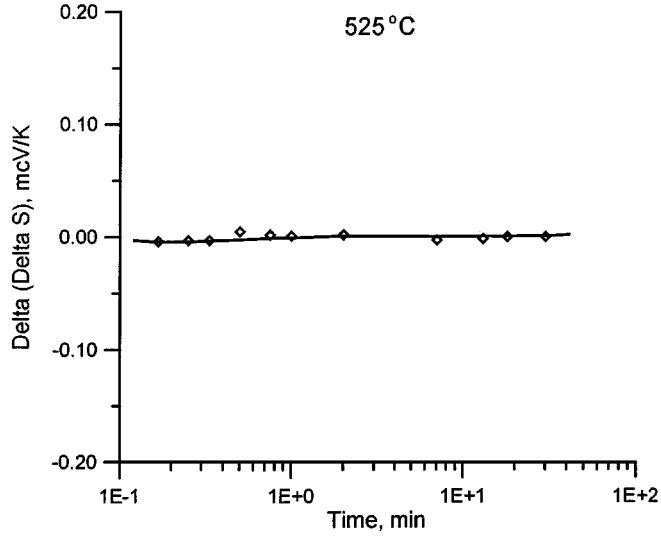

(f)

Figure 4 Kinetics of decomposition in alloys *1* and *2* (350 and 450 °C) studied by thermoelectric power measurements.

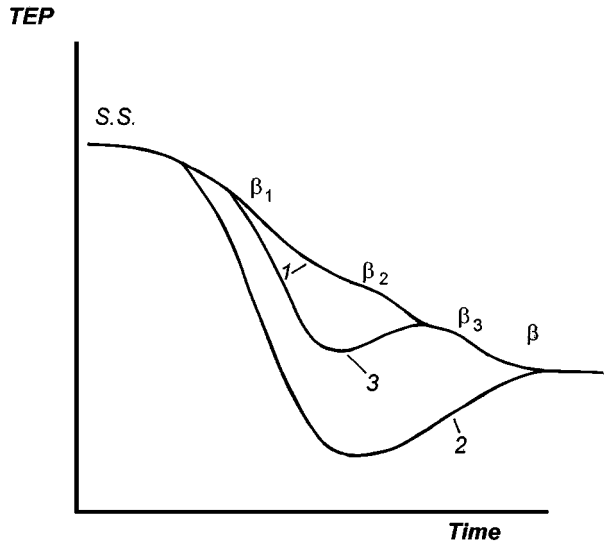

Figure 5 Possible variants of TEP variation upon decomposition of supersaturated solid solution in Al–Mg–Si alloys.

curve *3* in Fig. 4. Before the maximum, we observe the precipitation of β' and Si (Figs 3a–c and 4). After the maximum, we have particles of silicon, the precipitates of the equilibrium β phase (Fig. 3d and e) along with coarse and rather incoherent precipitates of intermediate in structure phase (Fig. 3f). These precipitates are still designated as β' (to distinguish them from the equilibrium cubic β phase) and have nearly the same composition as the equilibrium phase. The conclusion that the β' phase observed after the maximum in TEP curves has a composition close to that of the equilibrium β phase, results from the obvious fact that the TEP remains unchanged showing that the solid solution has reached its saturated concentration.

It seems worthy to underline once more that, according to TEM and TEP examinations, the formation of the equilibrium β phase and the virtually saturated solid solution does not exclude the coexistence of phases with nearly the same composition but intermediate structures. Arriving at a complete equilibrium may take a very long time (as has been noted by Wenstengen and Ryum [7]).

4.3. An S-curve for isothermal transformations in alloy *1*

Taking into account our experimental data on the kinetics of precipitation upon high-temperature anneals, it can be concluded that in the temperature range between 300 and 400 °C, the precipitation starts with the formation of the intermediate semi-coherent β' phase and Si. On further annealing, the β' particles grow, and then a stable (at least in the composition) incoherent phase forms. At above 400 °C and up to 525 °C, the equilibrium β phase precipitates directly from the solid solution without the formation of intermediate phases. This conclusion is based on the analysis of TEP curves obtained at high-temperature annealing and on reference data [7, 8]. When annealing at temperatures above 400 °C, any effects corresponding to the precipitation of semicoherent phases such as decrease and increase

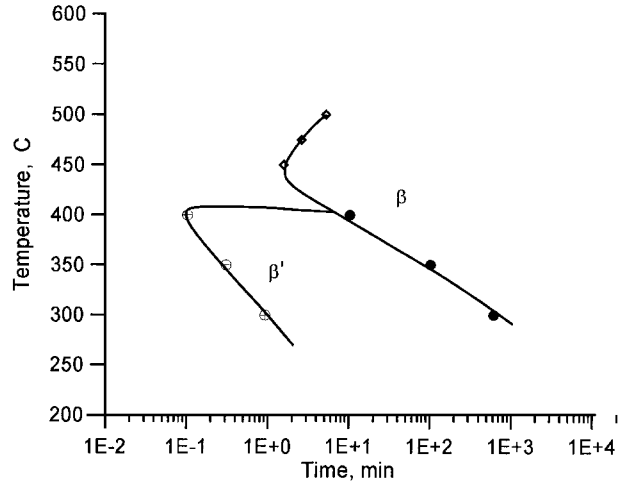

Figure 6 Isothermal transformation curve for alloy *1* (quenching directly to the temperature of annealing).

in TEP are not observed. The only effect observed is a TEP decrease and a stabilization, which reflects the precipitation of a Mg-rich phase.

The results obtained using isothermal anneals and TEM examinations suggest an S-curve (isothermal transformations) for the precipitation of β' and β phases in alloy *1* quenched directly to the temperature of annealing as shown in Fig. 6. The S-curve shows that the precipitation of β' phase can occur at rather high temperatures, up to 400 °C. In this case, it should be noted that the term "β'" phase is understood as a series of phases with a structure different to that of the equilibrium β phase. The stability of the β' phase up to such high temperatures in Al–Mg–Si alloys quenched at considerably low cooling rates was previously reported by Wenstengen and Ryum [7].

5. Conclusions

1. The high-temperature decomposition of supersaturated solid solutions in Al–Mg–Si alloys with an excess of silicon occurs either by the formation of an intermediate β' phase (at 300–400 °C), which is later gradually replaced by the equilibrium Mg_2Si phase or (above 400 °C and up to 500 °C) by direct precipitation of the equilibrium phase. Simultaneously, silicon precipitates during annealing forming its own particles.

2. Decomposition starts with the precipitation of a semi-coherent intermediate phase even at a temperature as high as 400 °C.

3. At temperatures below 400 °C, the stable composition of the solid solution is obtained after the formation of the β phase. However, the appearance of the equilibrium phase does not exclude the coexistence of coarse particles with a nonequilibrium structure but close to an equilibrium composition.

4. The formation of the equilibrium β phase probably occurs independently while particles of an intermediate phase are dissolving.

5. Two types of intermediate phase structures were observed in the examined alloys. These are β' phases of the C and A types previously reported by Matsuda *et al.* [4]. The reason for which this or that phase precipitates is not yet understood.

Acknowledgements

The authors would like to thank Péchiney-Voreppe for supplying alloys, Dr. C. Sigli from Péchiney-Voreppe for discussions, and Mr. J. Bigot for preparation of samples for TEP measurements.

References

1. J. E. HATCH (Ed.) "Aluminum. Properties and Physical Metallurgy" (ASM, Metals Park, 1984).
2. M. H. JACOBS, *Philos. Mag.* **26** (7) (1972) 1.
3. J. P. LYNCH, L. M. BROWN and M. H. JACOBS, *Acta Metall.* **30** (1982) 1389.
4. K. MATSUDA, S. IKENO, T. SATO and A KAMIO, in Proceedings of the 5th International Conference on Aluminium Alloys, Grenoble, 1996, edited by J. H. Driver, B. Dubost, F. Durant *et al*. (Transtec Publications, Zuerich) *Mater. Sci. Forum* **217–222** (1996), pp. 707–712.
5. K. MATSUDA, S. TADA, S. IKENO and A. KAMIO, in Proceedings of the 4th International Conference on Aluminum Alloys: Their Physical and Mechanical Properties, Atlanta, 1994, edited by T. H. Sanders, Jr and E. A. Starke, Jr. (Georgia Institute of Technology, Atlanta, 1994) **1**, pp. 598–604.
6. K. MATSUDA, S. IKENO, T. SATO and A. KAMIO, *Scr. Mater.* **34** (11) (1996) 1797.
7. H. WESTENGEN and N. RYUM, *Z. Metallkde.* **70** (8) (1979) 528.
8. N. MARUYAMA, R. UEMORI, N. HASHIMOTO, M. SAGA and M. KIKUCHI, *Scr. Mater.* **36** (1) (1997) 89.
9. R. BORELLY, P. MERLE and D. ADENIS, in "Light Metals," edited by P. G. Campbell (TMS, Warrendale, 1989), pp. 703–712.
10. D. DAFIR, PhD thesis, INSA de Lyon (1993).
11. S. M. SEYED REIHANI, D. DAFIR and P. MERLE, *Scr. Metall. Mater.* **28** (5) (1993) 639.

Received 8 September 1997
and accepted 27 August 1998